with superoxide radicals than do fully chelated complexes. Accumulating evidence supports an earlier suggestion by Fee[31] that the rate-determining step in the overall mechanism may be the rate at which a liganded water/OH^- is exchanged for an O_2^-. For example, only one, ($CuHist_2H^{3+}$), out of six Cu(II)-histidine complexes known to exist in the pH range between 1 and 10 disproportionates superoxide radicals. This particular complex is known to have an exchangeable water molecule. Also, Fe(II)-EDTA has a coordinated OH^- ligand in the pH range 9-11.8 which can be exchanged with an O_2^- radical, this forming a Fe(II)-EDTA-O_2^- complex.[32,33]

The present study shows that although all four Cu(II)-arginine complexes that exist between pH 1.5 and 12.5 dismutate HO_2/O_2^-, the truly efficient ones are those two ($CuArgH^{2+}$ and $CuArg^+$) complexes that have only one arginine ligand, the other sites being occupied most likely with exchangable water or OH^- ions. The result of this selective reactivity, in both this and the Cu(II)-histidine system, is that these complexes carry out very facile reactions with superoxide over narrow pH ranges. This suggests that SOD may be biologically significant not only because it dismutates O_2^- at a diffusion-controlled rate but also because that rate is invariant of pH (pH 4.5-11).

The earlier study of the Cu(II)-histidine system led to the conclusion that the reactive complex, $CuHist_2H^{3+}$, did not form an observable transient with HO_2/O_2^-. In the present study, which is the first in which the reactivity of O_2^- with metal complexes was studied at high O_2 concentrations (0.16 M), again no HO_2/O_2^- complexes were observed when both Cu_{aq}^{2+} and Cu(II)-histidine were reacted with O_2^-. However, Cu(II)-arginine complexes were shown, in the presence of high O_2 concentration, to react through the formation of a CuO_2^+ intermediate. While these Cu(II)-arginine complexes should not be taken as model systems for superoxide dismutases, for which theoretical studies have advanced a hypothesis suggesting that the amino end of the arginine-141 group stabilizes an O_2^- bound to the copper in the active site (which is complexed by imidazole moieties), they show that O_2^- can be complexed by certain copper complexes, thus supporting the above hypothesis.

As postulated previously, the formation of a superoxide–copper complex in SOD may indeed be the answer to some complex structural and thermodynamic requirements for the efficient operation of the catalytic cycle.

Acknowledgment. We acknowledge helpful discussions with Drs. K. Sehested and E. Bjergbakke. This work was supported by NIH Grant R01GM23658-10 and carried out at Risø National Laboratory, Denmark, and Brookhaven National Laboratory, which is operated under contract DE-AC02-76CH00016 with the U.S. Department of Energy. One of us (D.E.C.) thanks the staff of the Accelerator Department of Risø for their kindness and help during her stay there.

Registry No. $CuArgH^{2+}$, 108101-05-9; $Cu(ArgH)_2^{2+}$, 28471-34-3; $CuArg_2H^+$, 108101-06-0; $CuArg^+$, 97972-87-7; O_2^-, 11062-77-4.

(31) Fee, J. A. In *Metal Ions in Biological Systems*; Sigel, H., Ed.; Marcel Dekker, Inc.: New York, 1981; Vol. 13, pp 259–298.
(32) Ilan, Y. A.; Czapski, G. *Biochim. Biophys. Acta* **1977**, *498*, 386.
(33) Bull, C.; Fee, J. A.; O'Neill, P.; Fielden, E. M. *Arch. Biochem. Biophys.* **1982**, *215*, 551.

EXAFS and Near-Edge Structure in the Cobalt K-Edge Absorption Spectra of Metal Carbonyl Complexes

Norman Binsted,[1a] Stephen L. Cook,[1a] John Evans,*[1a] G. Neville Greaves,[1b] and Richard J. Price[1a]

Contribution from the Department of Chemistry, The University, Southampton SO9 5NH, UK, and the SERC Daresbury Laboratory, Daresbury, Warrington WA4 4AD, UK.
Received November 20, 1986

Abstract: EXAFS data of the Co K-edges of $PPN[Co(CO)_4]$ (**1**), $Co_3(CO)_9CH$ (**2**), and $Co_4(CO)_{10}(PPh)_2$ (**3**) have been analyzed. A spherical wave theory using ab initio phase shifts and including multiple scattering to third order allows structural parameters to be accurately obtained. Distances were determined to within 0.03 Å with use of data from 14 eV above the absorption edge. This method can also provide an estimate of the mean Co–C–O angle, but an attempt to reproduce multiple scattering effects with a variable coordination number and phase parameter was unreliable in this regard. Intraligand multiple scattering is dominant in these complexes. Statistical criteria for limiting the number of refinable parameters in a multi-shell system are also presented. Pre- and near-edge features may be used qualitatively to fingerprint the cobalt environments in these complexes.

Previously we have used EXAFS to identify the structures of metal carbonyl clusters[2] and to study the chemistry of clusters on functionalized and nonfunctionalized oxide surfaces.[3-5] While these treatments employed a spherical wave formalism,[6] using a computationally fast algorithm suitable for polycrystalline or amorphous samples,[7] rather than the more commonly used plane wave approximation,[8] they were restricted to single scattering events. Although multiple scattering is most important at low

(1) (a) University of Southampton. (b) Daresbury Laboratory.
(2) Cook, S. L.; Evans, J.; Greaves, G. N.; Johnson, B. F. G.; Lewis, J.; Raithby, P. R.; Wells, P. B.; Worthington, P. *J. Chem. Soc., Chem. Commun.* **1983**, 777.
(3) Cook, S. L.; Evans, J.; Greaves, G. N. *J. Chem. Soc., Chem. Commun.* **1983**, 1288.
(4) Binsted, N.; Cook, S. L.; Evans, J.; Greaves, G. N. *J. Chem. Soc., Chem. Commun.* **1985**, 1103.
(5) Cook, S. L.; Evans, J.; Greaves, G. N.; McNulty, G. S. *J. Chem. Soc., Dalton Trans.* **1986**, 7.
(6) Lee, P. A.; Pendry, J. B. *Phys. Rev. B* **1975**, *11*, 2795.
(7) Gurman, S. J.; Binsted, N.; Ross, I. *J. Phys. C* **1984**, *17*, 143.
(8) Sayers, D. E.; Stern, E. A.; Lytle, F. W. *Phys. Rev. Lett.* **1971**, *27*, 1204. Halaka, F. G.; Boland, J. J.; Baldeschwieler, J. D. *J. Am. Chem. Soc.* **1984**, *106*, 5408. Tohji, K.; Udagawa, Y.; Tanabe, S.; Ida, T.; Uedo, A. *J. Am. Chem. Soc.* **1984**, *106*, 5172. Sinfelt, J. H.; Via, G. H.; Lytle, F. W.; Greegor, R. B. *J. Chem. Phys.* **1981**, *75*, 5527. Meitzner, G.; Via, G. H.; Lytle, F. W.; Sinfelt, J. H. *J. Chem. Phys.* **1983**, *78*, 2533. Van't Blik, H. F. J.; van Zon, J. B. A. D.; Huizinga, T.; Vis, J. C.; Koningsberger, D. C.; Prins, R. *J. Am. Chem. Soc.* **1985**, *107*, 3139. Van Zon, J. B. A. D.; Koningsberger, D. C.; van't Blik, H. F. J.; Sayers, D. E. *J. Chem. Phys.* **1985**, *82*, 5742.

0002-7863/87/1509-3669$01.50/0

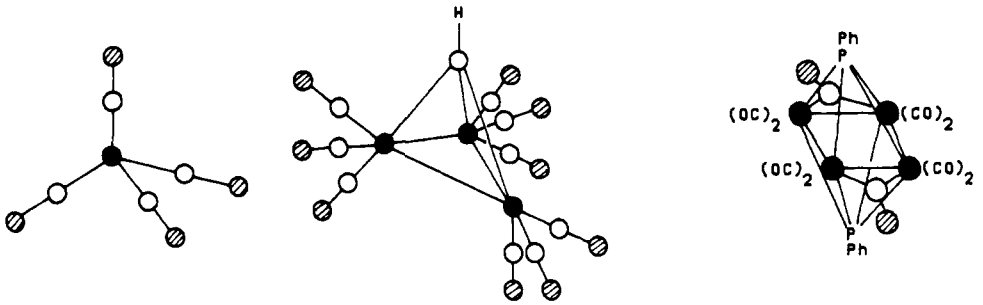

Figure 1. Structure of the cobalt species in $PPN[Co(CO)_4]$ (**1**), $Co_3(CO)_9CH$ (**2**), and $Co_4(CO)_{10}(PPh)_2$ (**3**). Cobalt, oxygen, and carbon atoms are shown as filled, hatched, and open circles, respectively.

photoelectron energies, strong multiple scattering effects extend to higher energies in the case of colinear atomic arrays.[6] Indeed considerable enhancement of the oxygen backscattering in $Mo(CO)_6$ was noted several years ago.[9] We have therefore extended the analysis procedures to include multiple scattering. Inclusion of terms involving double and triple scattering, particularly within the terminal carbonyl groups, will therefore improve the accuracy of the EXAFS analyses and permit us to treat the lower photoelectron energies where the signal-to-noise ratio is highest. In addition, it may be possible to exploit the strong angular dependence of multiple scattering terms in order to determine some bond angles without the use of single crystal/polarized beam techniques.[10-12]

Three model compounds were chosen as examples of metal carbonyl complexes of differing complexity all of which have been characterized by single-crystal diffraction studies. These were a simple high-symmetry mononuclear complex, $(PPN)[Co(CO)_4]$ (**1**),[13] a small, symmetrical cluster, $(\mu_3\text{-}CH)Co_3(CO)_9$ (**2**),[14] and a larger cluster in which there is a nonbonded metal-metal distance, $(\mu_4\text{-}PPh)_2Co_4(\mu\text{-}CO)_2(CO)_8$ (**3**)[15] (Figure 1). In this report we present analyses of the cobalt K-edge EXAFS of these compounds, paying particular attention to the importance of multiple scattering within the Co–C–O groups and the relative importance of higher order paths between the C–O ligands. Additionally we have been concerned to establish the degree to which the EXAFS formalism can be extended back toward the absorption edge and also to delineate the information content of EXAFS data. Most previous studies of multiple scattering have utilized a plane wave theory,[10-12,16-19] but this has resulted in significant errors in the phase of the multiple scattering contributions in metal carbonyl complexes.[20] We therefore maintain the spherical wave formalism in these analyses. We also report some qualitative relations between the near-edge structure of some cobalt complexes and the local metal environment.

Experimental and Data Reduction

Spectra were obtained from powdered samples measured in transmission mode on Beam Line 7 on the Synchrotron Radiation Source of the SERC Daresbury Laboratory.

After background subtraction the spectra were Fourier filtered with use of a window broad enough to include all significant structure (about 0.9–3.8 Å), in order to remove noise and traces of residual background which might impede refinement. Fourier filtering also ensures that high order multiple scattering terms and contributions from remote shells are removed and produces a spectrum with equal intervals in k space. For the spectrum of **3**, we estimated the distortion produced by Fourier filtering by repeating the procedure on the filtered spectrum. We then computed the difference between the two k^3 weighted spectra which we found to be less than 2% of the total area, mainly associated with the first and last few points. This is smaller than the effect of residual background and the lack of fit between theory and experiment so it would not seriously affect our results. The range of data we refined (from about 14 to about 550 eV above the edge) was limited at low energy by difficulties in background subtraction and Fourier filtering and at high energy by noise and monochromator glitches. We took the edge position to be the location of the maximum in the first derivative, which was found to be above the half-height of the edge. For these spectra, which do not possess a strong white line, we assume that this is just above the vacuum zero level.

Theory and Analysis

For all our calculations we used the spherical wave theory of Lee and Pendry,[6] employing computationally fast algorithms suitable for polycrystalline or amorphous samples.[7,20] The use of spherical wave rather than the much faster plane wave theory is essential when calculating multiple scattering for systems with bond lengths as short as the C–O bond (ca. 1.15 Å) even at energies as high as several keV.[20] We used 13 phaseshifts in calculating single and double scattering as well as in calculating the strong forward scattering term for the triple scattering contributions; for the third-order backscattering term 10 phaseshifts were used. This is entirely satisfactory for the low atomic numbers and energy range in question. Phaseshifts for each element were calculated according to the prescription of Loucks[21] using the muffin-tin approximation to the potentials in the solid.[22] Atomic wave functions were calculated self-consistently with a relativistic Hartree–Fock program with Slater exchange.[23] The central atom phaseshifts included the effect of the core hole as prescribed by the final state rule.[24] We calculated the excited atom wave function for an atom with a 1s hole and in which the outer electrons are fully relaxed to the presence to the core hole, which should approximate to the situation at low photoelectron energies.[25] To assess the possible effect of the stronger potential seen by a higher energy photoelectron (incomplete screening and relaxation[26]), we fitted the spectra with $Z + 1$ phaseshifts (with screened core hole). Even this extreme variation in potential had little effect on the results (distances were 0.01–0.02 Å shorter), so we conclude that how the core hole is treated is not critical in this case. The muffin-tin zero potentials gave a volume average (for **2**) of −18 eV, the same as the base of the valence band.[27] The spread of zero potential values of the elements studied of about 6 eV is not ideal, and adjusting the muffin-tin radii to ensure a common origin

(9) Cramer, S. P.; Hodgson, K. O.; Stiefel, E. I.; Newton, W. E. *J. Am. Chem. Soc.* **1978**, *100*, 2748.
(10) Teo, B. In *EXAFS Spectroscopy*; Teo, B., Joy, D. C., Eds.; Plenum: New York, 1981.
(11) Teo, B. *J. Am. Chem. Soc.* **1981**, *103*, 3990.
(12) Co, M. S.; Hendrickson, W. A.; Hodgson, K. O.; Doniach, S. *J. Am. Chem. Soc.* **1983**, *105*, 1144.
(13) Chiang, J. MS Thesis, University of Southern California, 1974. Bau, R. B., personal communication.
(14) Leung, P.; Coppens, R.; McMullan, R. K.; Koetzle, T. F. *Acta Crystallogr. B* **1981**, *37*, 1347.
(15) Ryan, R. C.; Dahl, L. F. *J. Am. Chem. Soc.* **1975**, *97*, 6904.
(16) Alberding, N.; Crozier, E. D. *Phys. Rev. B* **1983**, *27*, 3374.
(17) Boland, J. J.; Baldeschwieler, J. D. *J. Chem. Phys.* **1984**, *80*, 3005.
(18) Boland, J. J.; Baldeschwieler, J. D. *J. Chem. Phys.* **1984**, *81*, 1145.
(19) Biebesheimer, V. A.; Marques, E. C.; Sandstrom, D. R.; Lytle, F. W.; Greegor, R. B. *J. Chem. Phys.* **1981**, *81*, 2599.
(20) Gurman, S. J.; Binsted, N.; Ross, I. *J. Phys. C* **1986**, *19*, 1845.
(21) Loucks, T. *The Augmented Plane Wave Method*; Benjamin: New York, 1967.
(22) Mattheis, L. F.; *Phys. Rev. A* **1964**, *133*, 1399.
(23) Program by Desclaux, J. P., modified by Durham, P. J.
(24) von Barth, U.; Grossman, G. *Phys. Rev. B* **1982**, *25*, 5150.
(25) Lee, P. A.; Beni, G. *Phys. Rev. B* **1977**, *15*, 2862.
(26) Hayes, T. M.; Boyce, J. B. *Solid State Phys.* **1981**, *37*, 173.
(27) Costa, N. C. V.; Lloyd, D. R.; Brint, P.; Pelin, W. K.; Spalding, T. R. *J. Chem. Soc., Dalton Trans.* **1982**, 201.

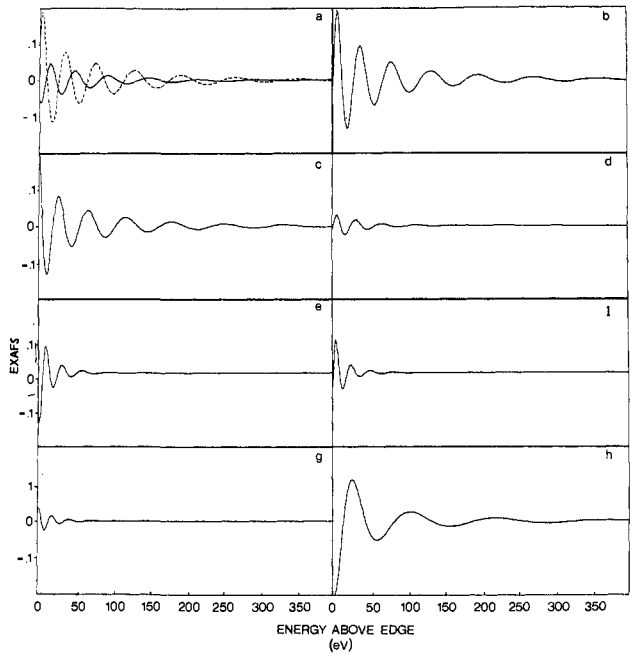

Figure 2. Calculated contributions of the scattering paths for $Co(CO)_4^-$ using the parameters in Table IA: (a) 4 × Co–O–Co (solid), sum of (a), (b), and (c) (broken); (b) 4 × Co–O–C–Co + 4 × Co–C–O–Co; (c) 4 × Co–C–O–C–Co; (d) 12 × Co–C–C–Co; (e) 4 × Co–O–C–O–C–Co + 4 × Co–C–O–C–O–Co; (f) 4 × Co–C–O–C–O–C–Co; (g) 4 × Co–O–C–O–Co; (h) 4 × Co–C–Co.

for all the phaseshifts might improve our fits. This is, however, by no means certain in view of the considerable approximations involved in representing molecular systems by spherically averaged potentials. In order to model inelastic processes a constant imaginary potential[28] of −2.5 eV was used. This is physically realistic in view of the longer core hole lifetimes expected from insulators as compared to metals[29] and gave good results with all three spectra. The reduction in amplitude due to multiple excitations etc. was accounted for by a constant factor of 0.7.

Analysis involved least-squares minimization of the term[30]

$$\sum_i (k^3(\chi_i^T - \chi_i^E))^2$$

where χ_i^T and χ_i^E are the theoretical and experimental EXAFS, respectively. However, the results of refinements are reported in terms of the discrepancy index

$$R = \int |(\chi^T(k) - \chi^E(k))| k^3 \, dk / \int |\chi^E(k)| k^3 \, dk \times 100\%$$

which is independent of the sampling intervals and of the absolute amplitude of the spectrum. Statistical errors and correlation coefficients are calculated by standard techniques[31] with use of a numerical estimate of the Jacobian matrix. We note, however, that the variances can only be regarded as crude estimates in view of the strong correlations between certain variables.[32]

Results and Discussion

Multiple Scattering Contributions. The relative importance of the different orders of scattering is illustrated in Figure 2, which presents calculated spectra for (PPN)[$Co(CO)_4$] (**1**) from just below the edge to about 400 eV. The double and triple scattering terms (b and c) are in this case more important than the oxygen shell single scattering term (a) and so demonstrate the necessity

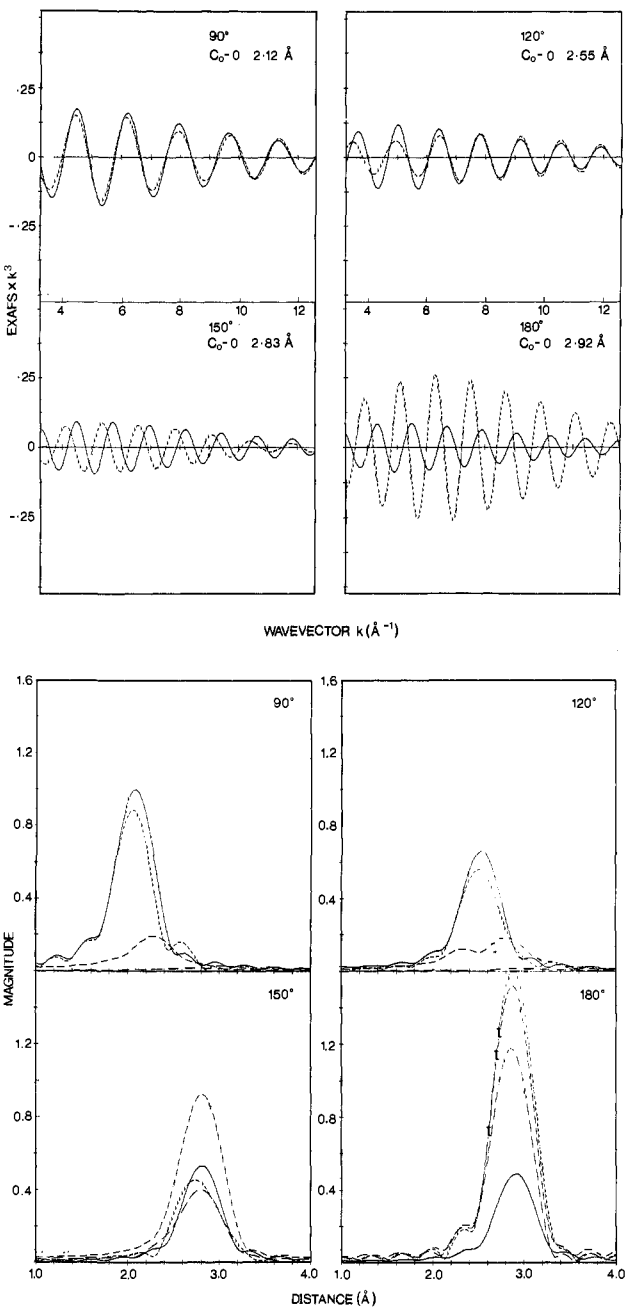

Figure 3. Oxygen shell contributions to $k^3\psi(k)$ (upper) and the Fourier transform (lower) for a Co–C–O unit. Parameters as in Table IA excepting for the bond angle and Co–O distance (as shown) (- -) total contribution, (—) single scattering, (– –) double scattering, and (— — —) triple scattering.

of taking multiple scattering into account. The higher order terms (4th and 5th order) are subordinate and negligible except within about 10 eV of the edge (paths e, f, and g all have the same path length but differ in phase and so partial cancellation occurs as with paths a, b, and c). As multiple scattering will always be most important when, as here, there are strong forward scattering terms involved, we can be sure that a multiple scattering theory including contributions up to third order will be adequate in describing molecular spectra except where more than three atoms are colinear (or nearly so) when 4th order terms may be required (as in some thiocyanates and possibly some paths in certain ring structures). Even in close packed metals, although multiple scattering is undoubtedly more important, the greater atomic radii, the shorter core hole lifetimes, and the restriction of paths involving strong focussing effects to 4th or higher shells will reduce the amplitude of higher order paths. So our approach of calculating specific paths, which has the advantage of being applicable to both high-

(28) Pendry, J. B. *Low Energy Electron Diffraction*; Academic Press: London, 1974.
(29) Gurman, S. J. *J. Phys. C* **1983**, *16*, 2987.
(30) Modification of the Harwell Laboratory routine VAOSA.
(31) Cox, A. D. In. *EXAFS for Inorganic Systems*; Garner, C. D., Hasnain, S. S., Eds.; DL/SCI/R17, 1981; p 51.
(32) Brandt, S. *Statistical and Computational Methods in Data Analysis*; North Holland: Amsterdam, 1970.

Table I. Optimum Parameters Using All Shells up to 3.8 Å with (1) Multiple Scattering Theory, (2) Single Scattering Only, (3) Single Scattering with Variable Phase (P) and Occupation Number (N) for Oxygen[a]

A. $Co(CO)_4^-$

	X-ray		1 E_0 = 27.0 (2); R = 17.0		2 E_0 = 30.8 (13); R = 54.2		3 E_0 = 26.5 (4); R = 15.0 N_0 = 10.7 (3); P = 156 (6)	
	N	R (Å)	R (Å)	A (Å^2)	R (Å)	A (Å^2)	R (Å)	A (Å^2)
C	4	1.74	1.77 (0)	0.005 (0)	1.75 (1)	0.005 (1)	1.77 (0)	0.005 (0)
O	4	2.89	2.92 (0)	0.009 (0)	3.02 (1)	0.000 (1)	2.78 (1)	0.006 (0)

B. $Co_3(CO)_9CH$

	X-ray		E_0 = 27.1 (1); R = 11.1		E_0 = 17.6 (10); R = 43.4		E_0 = 26.9 (4); R = 8.5 N_0 = 6.4 (3); P = 150 (8)	
	N	R (Å)	R (Å)	A (Å^2)	R (Å)	A (Å^2)	R (Å)	A (Å^2)
C_{CO}	3	1.81	1.81 (2)	0.009 (1)	1.86 (1)	0.004 (1)	1.81 (0)	0.008 (3)
C_{CH}	1	1.89	1.86 (7)	0.012 (13)	2.07 (3)	0.003 (5)	1.87 (7)	0.008 (10)
Co	2	2.48	2.46 (0)	0.008 (0)	2.51 (1)	0.005 (1)	2.47 (0)	0.008 (0)
O	3	2.95	2.94 (0)	0.011 (0)	2.70 (1)	0.001 (2)	2.90 (1)	0.005 (0)
C	4	3.29	3.37 (1)	0.023 (3)	3.27 (3)	0.25 (9)	3.34 (5)	0.089 (25)

C. $Co_4(CO)_{10}(PPh)_2$[b]

	X-ray		E_0 = 27.7 (7); R = 7.9		E_0 = 22.1 (20); R = 16.1		E_0 = 28.3 (12); R = 8.6 N_0 = 6.3 (21); P = 155 (3)	
	N	R (Å)	R (Å)	A (Å^2)	R (Å)	A (Å^2)	R (Å)	A (Å^2)
C_T	2	1.80	1.79 (1)	0.005 (3)	1.83 (1)	0.007 (4)	1.79 (1)	0.006 (5)
C_B	1	1.94	1.93 (2)	0.006 (12)	2.03 (9)	0.005 (32)	1.92 (5)	0.007 (25)
P	2	2.24	2.23 (1)	0.009 (3)	2.27 (5)	0.008 (10)	2.22 (2)	0.009 (6)
Co_{BR}	1	2.52	2.51 (7)	0.009 (3)	2.67 (25)	0.010 (80)	2.51 (7)	0.009 (20)
Co_{NB}	1	2.70	2.71 (2)	0.007 (4)	2.77 (17)	0.004 (39)	2.72 (18)	0.006 (29)
O_T	2	2.92	2.91 (4)	0.018 (6)	2.53 (10)	0.010 (58)	2.85 (19)	0.016 (129)
O_B	1	2.97	2.96 (22)	0.023 (49)	3.05 (16)	0.15 (84)	2.96 (172)	0.019 (470)
C	2	3.5	3.46 (1)	0.005 (3)	3.47 (5)	0.19 (13)	3.46 (2)	0.003 (9)
Co_D	1	3.69	3.65 (1)	0.012 (1)	3.68 (2)	0.015 (3)	3.65 (1)	0.11 (3)

[a] A is the Debye Waller factor $2\sigma^2$. The discrepancy index R is defined in the text. [b] Subscripts: T = terminal, B = bridging, BR = bridged Co–Co bond, NB = nonbridged Co–Co bond, D = diagonal Co--Co distance across the Co_4 rectangle.

and low-energy regions, may account for much of the structure for which a full multiple scattering theory[12] is normally used.

Figure 2 also illustrates the relative importance of scattering within the carbonyl groups compared to scattering between the carbonyl groups (paths Co–C–C–Co). It is apparent that the interligand paths are of much less importance even in this highly symmetric structure and could in general be neglected except in close-packed structures.

Angular Dependence. The angle dependence of multiple scattering within a Co–C–O unit is demonstrated in Figure 3. Here a constant Co–C and C–O bond length is assumed, and the Co---O distance is allowed to vary as the Co–C–O bond angle changes from 90 to 180°. The resulting Co---O distances are not of course chemically realistic except in the 180° case.

With a 90° bond angle, the effect of multiple scattering is limited to a slight amplitude reduction. At 120° there is a marked amplitude reduction, but at low energy only. The 150° case shows little change in amplitude but a large retardation of the phase of the oscillations and a small change in apparent Co--O distance as shown by the Fourier transform. Only in the 180° case do we see the strong enhancement in amplitude normally associated with multiple scattering (together with a change in phase), in apparent Co---O distance (by about 0.04 Å) and in the energy dependence of the amplitude (apparent Debye–Waller factor). We conclude that multiple scattering is always going to have an important influence on the contribution of carbonyl groups to the EXAFS spectrum, although for bridging groups with bond angle of 135 to 150° this may be a reduction in amplitude or a change in phase rather than an enhancement of the peak as observed with terminal carbonyls.

Curve Fitting. Analysis of the three spectra by least-squares refinement yielded optimum values for the radial distance of an atomic shell (R) and for the Gaussian Debye–Waller term $A = 2\sigma^2$, as well as the magnitude of the photoelectron energy at $k = 0$ (E_0), which should represent the average potential in the crystal. Some additional parameters were also included as described below. Initially we refined parameters for all the shells present in the crystal within the range of the Fourier filtered data. The nonbonding carbon shells, however, include a considerable spread of distances. Table I shows the results of three refinements: (1) using the multiple scattering theory, including multiple scattering within the carbonyl groups and for **1** between the carbonyl groups (double scattering paths involving the bridging methylidyne carbon in **2** and the phosphorus atoms in the bridging PPh in **3** have therefore been excluded); crystallographic occupation numbers and bond angles were assumed (Co–C–O angles of 180° and 145° for terminal bridging carbonyl groups, respectively; 109.47° for the C–Co–C angle in **1**); (2) using a single scattering theory and still assuming the crystallographic occupation numbers; and (3) using the single scattering theory but with an additional phase included in the contribution of the oxygen shell associated with the terminal carbonyl groups; the additional phase and the occupation number of the terminal carbonyl oxygen shell were included in the refinement.

The fits obtained for each case are shown in Figure 4.

A good fit to all three spectra and their Fourier transforms was obtained by using the multiple scattering theory (R = 8% to 17%) with a good approximation to the crystallographic distances. (At within 0.03 Å for major shells this is about the accuracy expected in view of systematic errors associated with phaseshifts.) The values of E_0 obtained (all about 27 eV), are equivalent to an energy about 9 eV below the muffin-tin zero. This is rather low but not unreasonable for compounds in which a strong departure from spherically symmetric potentials occurs. The Debye–Waller factors for the nonbonding carbon shells in **2** and **3** are too low to be realistic, and those for the adjacent oxygen shell are correspondingly high, indicating some compensatory effect.

Use of the single scattering theory in the second refinement failed to give a good fit to **1** and **2** although the fit to **3**, where there were more variables, was acceptable. The best fit parameters associated with the oxygen shells are also unrealistic, confirming the inability of the single scattering theory to fit these spectra.

Table II. Correlations between Variables Associated with All Shells up to 3.8 Å Using Multiple Scattering Theory[a]

A. $Co(CO)_4^-$

	R_1	R_2	A_1	A_2
R_2	0.33			
A_1	−0.05	0.06		
A_2	−0.02	−0.03	−0.02	
E_0	−0.50	−0.75	−0.02	0.00

B. $Co_3(CO)_9CH$

	R_1	R_2	R_3	R_4	R_5	A_1	A_2	A_3	A_4	A_5
R_2	−0.99									
R_3	0.58	−0.52								
R_4	−0.60	0.63	−0.10							
R_5	−0.19	0.21	0.06	0.39						
A_1	0.50	−0.62	0.07	−0.34	−0.14					
A_2	0.98	−0.94	0.60	−0.61	−0.19	0.35				
A_3	0.06	−0.08	0.03	0.16	0.07	0.22	0.00			
A_4	−0.40	0.37	−0.43	0.16	0.02	−0.07	−0.42	−0.12		
A_5	−0.03	0.00	−0.14	−0.11	−0.13	0.05	−0.03	−0.07	0.14	
E_0	−0.02	−0.08	−0.48	−0.51	−0.37	0.29	−0.04	−0.09	0.10	0.24

C. $Co_4(CO)_{10}(PPh)_2$

	R_1	R_2	R_3	R_4	R_5	R_6	R_7	R_8	R_9	A_1	A_2	A_3	A_4	A_5	A_6	A_7	A_8	A_9
R_2	−0.18																	
R_3	−0.68	0.78																
R_4	−0.60	0.44	0.74															
R_5	−0.80	0.27	0.75	0.74														
R_6	0.13	0.44	0.25	0.43	−0.24													
R_7	0.19	−0.46	−0.46	−0.68	−0.08	−0.93												
R_8	0.36	−0.03	−0.19	−0.21	−0.04	−0.32	0.44											
R_9	0.13	0.40	0.29	0.37	0.14	0.38	−0.34	0.49										
A_1	0.70	−0.80	−0.95	−0.75	−0.69	−0.31	0.52	0.24	−0.26									
A_2	0.82	−0.63	−0.94	−0.85	−0.80	−0.27	0.54	0.30	−0.22	0.96								
A_3	0.68	−0.48	−0.80	−0.98	−0.74	−0.45	0.70	0.29	−0.33	0.82	0.91							
A_4	−0.66	0.16	0.52	0.09	0.70	−0.63	0.42	−0.00	−0.19	−0.42	−0.46	−0.16						
A_5	0.27	−0.29	−0.42	−0.89	−0.41	−0.58	0.73	0.19	−0.36	0.49	0.56	0.81	0.34					
A_6	−0.41	0.13	0.35	0.76	0.46	0.30	−0.51	−0.35	0.03	−0.43	−0.52	−0.70	0.14	0.87				
A_7	0.13	0.52	0.34	0.28	−0.08	0.69	−0.60	0.12	0.60	−0.32	−0.26	−0.32	0.29	0.23	0.25			
A_8	−0.24	0.38	0.48	0.33	0.28	0.31	−0.37	−0.01	0.56	−0.41	−0.43	−0.39	0.20	0.09	0.14	0.57		
A_9	−0.38	0.21	0.40	0.36	0.29	0.28	−0.42	−0.57	−0.00	−0.38	−0.44	−0.43	0.18	0.19	0.15	0.21	0.53	
E_0	0.24	−0.75	−0.74	−0.81	−0.37	−0.74	0.81	0.11	−0.58	0.74	0.71	0.81	0.15	0.75	0.46	0.67	0.45	0.31

[a] R_n and A_n refer to the distances and Debye–Waller factors respectively for shell n. Shell sequence as for Table I.

Indeed, it had previously only been possible to fit EXAFS data of carbonyl complexes by using physically unrealistic parameters in calculating oxygen phaseshifts.[2]

In the third refinement, the use of a variable occupation number and additional phase for the oxygens associated with the terminal carbonyl groups allowed a good fit to be obtained to all the spectra. Previous workers considering multiple scattering effects in a plane-wave model have used phase and amplitude correction factors as indicators of bond angles.[11,12,16] In fact the phase correction allowed a slightly better fit to be obtained than with the multiple scattering theory for two of the spectra, suggesting that the origins of the phaseshifts are not quite compatible. The oxygen parameters are still in error, however, R and A being too low and N too high.

The good fits and generally realistic parameters obtained by using the multiple scattering theory disguise a degree of uncertainty in the structural parameters which is apparent from the estimates of the variances (Table I) and the correlation coefficients (Table II). In **1**, the simple structure ensures a unique fit and weak correlations except between E_0 and the radial distances. The precision of the parameters is therefore high. Indeed, we find the discrepancy between crystallographic and EXAFS results surprising in view of the accuracy of the C and O shell distances obtained in **2** and **3**. In contrast, the large number of shells in **2** and **3** give rise to strong correlations between parameters of adjacent shells. Examples from Table II are between R_1 and A_1 in **2** (C_{CO} and C_{CH} shells, respectively) and also between A_4 and R_5 in **3** (bridged and nonbridged cobalt, respectively). As a consequence statistical errors are much larger. Indeed, we find it possible to obtain quite good fits using other structural models which differ in the position of minor shells and which include unrealistic Debye–Waller factors. The convergence of the refinements is also slow. Including a large number of shells in a refinement of an unknown system may therefore not only impede refinement but also lead to an incorrect structure being assumed.

In order to limit the number of parameters either minor shells may be omitted or combined with other shells or else parameters may be constrained to take the same or correlated values (e.g., all the Debye–Waller factors for a particular atom type may be assumed to have the same value, or be determined by the same linear function of R). Here the number of shells was reduced by applying two criteria: (1) shells whose k-space integral is much less than 10% of the total k^3 weighted spectrum, that is where for shell n

$$\int k^3\chi^n(k)\,\mathrm{d}k \Big/ \int k^3\chi^E(k)\,\mathrm{d}k \times 100 \ll 10$$

or (2) shells which display correlations of >0.8 to parameters of adjacent shells are either excluded or combined with other shells.

It is appreciated that in tackling analysis of an unknown structure there may be independent physicochemical evidence for the existence of a particular shell; it may also be identifiable in the Fourier transform even though it contributes less than 10% of the total EXAFS. The best approach then may be inclusion as nonrefined parameters in a manner similar to refinements of benzene rings as rigid bodies or of fixing C–H distances in X-ray diffraction refinements.

Applying these criteria to **2** and **3** reduces the number of shells to 3 and 6, respectively. In **3** this implies treating both bridging and terminal carbonyl groups equivalently. The nonbonding Co shell is clearly defined and remains.

Two shells of similar type and equal occupation number and Debye–Waller factor will interfere destructively, so as to more or less cancel out at some wavevector: $k > 0.25(R_b + R_a)/(R_b$

Table III. Optimum Parameters for Major Shells Using Multiple Scattering Theory[a]

	N	R (Å) X-ray	R (Å) EXAFS	A (Å²)
		B. $Co_3(CO)_9CH$		
		E_0 = 27.7 (2); β = 180 (1); R = 13.1		
C	3	1.81	1.82 (2)	0.006 (0)
Co	2	2.48	2.46 (1)	0.008 (0)
O	3	2.95	2.94 (2)	0.011 (0)
		C. $Co_4(CO)_{10}(PPh)_2$		
		E_0 = 28.9 (4); β = 166 (2); R = 12.3		
C	3	1.85	1.81 (0)	0.013 (0)
P	2	2.24	2.22 (0)	0.008 (0)
Co_B	1	2.51	2.50 (1)	0.010 (2)
Co_{nb}	1	2.70	2.73 (2)	0.010 (2)
O	3	2.94	2.89 (1)	0.014 (3)
Co_D	1	3.69	3.65 (1)	0.019 (2)

[a] β is the Co–C–O bond angle (deg).

$- R_a$) (where R is in atomic units). For the two bonding cobalt shells in **3** this occurs around $k = 7$, well below k_{max}, thus preventing the two shells from being effectively represented as a single shell. Rather than combine the shells we then therefore reduce the extent of the correlations by refining these two shells with equal Debye–Waller factors.

Having thus reduced the number of parameters, bond angles were included in the refinement. For **1** a 180° bond angle was clearly preferred, so parameters are as for Table I. Parameters for **2** and **3** are shown in Table III, with correlations for all three spectra in Table IV. The lack of fit is not significantly worse than in the previous case, and the bond angles are in excellent agreement with crystallographic values (the average X-ray value for **3** is about 168°). The agreement may in part be fortuitous as it is not clear that an averaged bond angle will always reflect the crystallographic mean.

We must, however, accept the impossibility of distinguishing two populations of carbonyl groups as a limitation of the technique. Table IV shows that with the reduction in the number of parameters correlations for **2** are reduced to acceptable levels but, although the problem in **3** is much reduced, some strong correlations remain. These all involve the bonding cobalt shells: the shorter (bridged) bond contributes toward the peak dominated by phosphorus and the longer (nonbridged) one toward that dominated by the carbonyl oxygen atoms. As these shells contribute significantly to the spectrum the consequent uncertainty in their parameters must be accepted. Better experimental data extending to higher energies would of course increase the precision attained. An averaged distance will normally be weighted toward the shorter shell because of the $1/r^2$ dependence inherent in the theory. In the case of oxygen shell, however, the mean is shorter than either, although still within 0.03 Å of the dominant shell, which is here greatly enhanced by the multiple scattering. As the adjoining Co distance is rather long, some compensatory effect seems likely. The difficulty in resolving non-Gaussian distributions by curve fitting alone is another limitation which must lead to caution in interpreting shells where a high Debye–Waller factor is due to static disorder or variability in bond lengths and also in comparing mean values with those obtained by X-ray methods.

Bond Angle Determination. The possibility of accurate bond angle determination with use of a plane wave multiple scattering theory of EXAFS either with ab initio phaseshift[11,17] or by means of a calibrated scale of amplitude factors[12] has previously been demonstrated. However, even with a precise formulation of the asymptotic theory[33] with the correct angle dependent Debye–Waller factors[11] it has been observed that for transition-metal carbonyls the short bond lengths involved give rise to a considerable discrepancy in the phase, and, at low energy, in the amplitude, between the asymptotic and the exact spherical wave theory.[20] The error involved could be minimized by including an additional E_0 correction and an additional mean free path term in the refinement for each shell.[11,17] However, in our multishell approach to fitting, which does not rely on being able to extract individual shell contributions by Fourier filtering, the introduction of such additional parameters will limit the possibility of discriminating between several proposed structures which differ in the number or type of additional ligands. Correlation of parameters with a calibrated scale of intensities[12] would limit the systems studied to those that have been reliably calibrated. Potentially the two parameters N_0 and P (Table I), obtained from fitting with a single scattering theory employing a modified phase and amplitude, could be used. To test this possibility data for complex **3** were refined with the reduced number of parameters but including the oxygen shell occupation number and an additional phase. This gave an N_0 of 2.6, indicating an amplitude reduction and therefore a bond angle of less than about 150°, while the optimum phase of 176° was greater than that obtained for the terminal carbonyl groups. Indeed, good fits over a wide range of values for the additional phase can be obtained as a consequence of the very high correlation between P, E_0, and R. This method is therefore unreliable.

Although the bond angle (strictly the sine of the bond angle) is strongly correlated with other variables over certain ranges of values, the extent of the correlation varies strongly with bond angle and the minima are consequently well-defined. Unlike the errors in the phase term, therefore, the estimates of the variances in bond angle appear to be realistic. We conclude that there is a possibility of determining bond angles in transition-metal carbonyls using the exact spherical wave theory including multiple scattering to third order even in quite complex systems, but other approaches are of limited use. Additional advantages of this theory are the ability to utilize data to within a few eV of an absorption edge and to obtain distances and Debye–Waller factors for remote shells with a similar degree of precision as for nearest neighbor shells.

Edge Structure. Figure 5 shows the cobalt K-absorption edges for **1**, **2**, and **3** as well as those for $PPN[Ru_3Co(CO)_{13}]$ (**4**), an oxidized sample of $Co_3(CO)_9(\mu_3\text{-}CSiCl_3)$ on alumina (**5**), and $[Co(OH_2)_6](NO_3)_2$ (**6**).

The edge structure of the spectra can be described in terms of three components: (1) a pre-edge peak or shoulder at approximately the energy of the metal absorption edge due to dipole-induced transitions to empty orbitals of 1s → 4p character,[34-36] (2) a steep rise at the absorption edge which appproximately corresponds to the onset of transitions to the continuum at the vacuum level, and (3) oscillatory structure at higher energies, which, as described above, can be largely described by a third-order scattering theory but which will include higher order contributions very close to the edge.

The maximum in the first derivative for **1**, **2**, and **3** occurs at 7720+/−1 eV. However, the latter two complexes possess a shoulder at lower energy which precludes an accurate comparison of these edge positions. Although the calibration is less certain for the other spectra in Figure 5, the edge positions appear to occur at the same energy. This suggests little change in position with oxidation state and therefore no significant change in the core potential. Marked changes in edge shift with oxidation state have been observed for early transition metals[37-39] but are absent on the lead L(III) edge.[35]

The shoulder in **2** and **3** may reflect a greater degree of p-orbital involvement in this energy region which may be associated with

(33) Boland, J. J.; Crane, S. E.; Baldeschwieler, J. D. *J. Chem. Phys.* **1982**, *77*, 142.

(34) Agarwal, B. K. *X-ray Spectroscopy*; Springer Series in Optical Spectroscpy, No. 15: Heidelberg, 1979.

(35) Rao, K. J.; Wong, J. *J. Chem. Phys.* **1984**, *81*, 4832.

(36) Parratt, L. G. *Rev. Modern Phys.* **1959**, *31*, 616.

(37) Bianconi, A. In *EXAFS for Inorganic Systems*; Garner, C. D., Hasnain, S. S., Eds.; DL/SCI.R17, 1981; p 13.

(38) Binsted, N.; Greaves, G. N.; Henderson, C. M. B. *Prog. Exp. Pet.* **1984**, *D25*, 6, 59 (NERC).

(39) Grunes, L. A. *Phys. Rev. B* **1983**, *27*, 2111. These data were reconsidered with the definition of the edge position as the maximum of the first derivative.

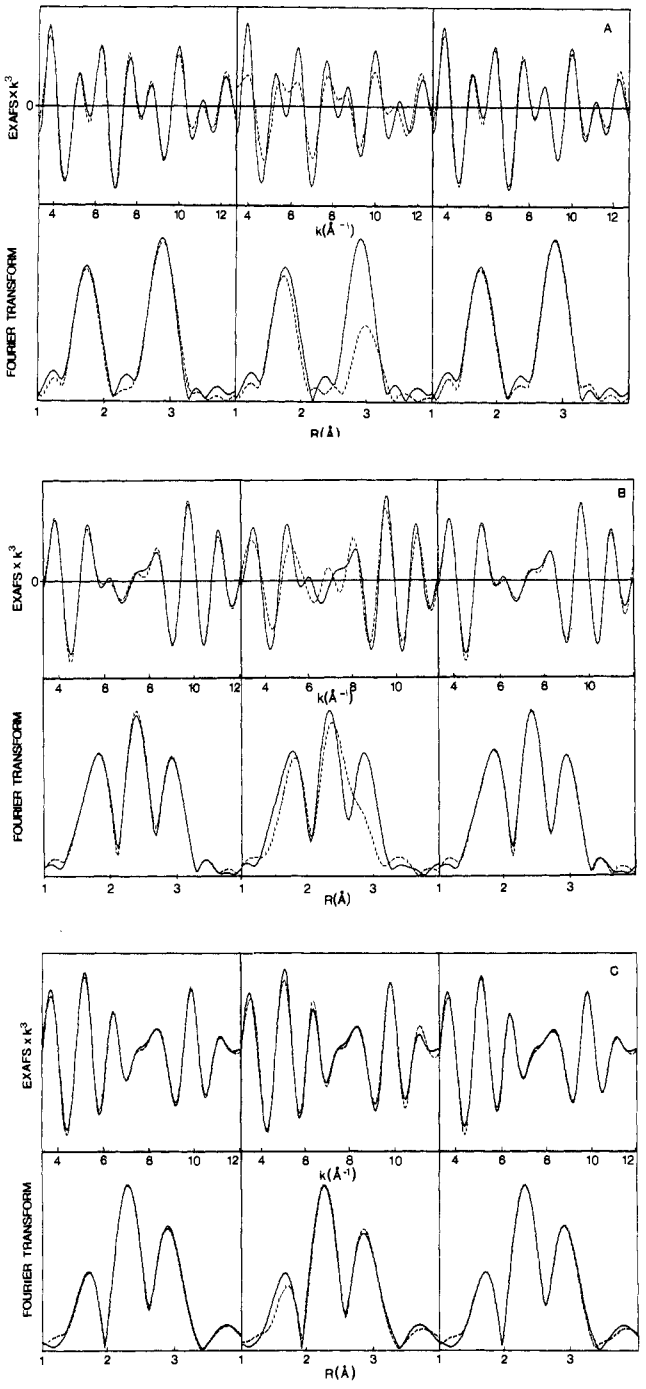

Figure 4. Three methods for fitting the Co K-edge EXAFS shown (with Fourier transforms) for (A) PPN[$Co(CO)_4$] (**1**), (B) $Co_3(CO)_9CH$ (**2**), and (C) $Co_4(CO)_{10}(PPh)_2$ (**3**). Left by multiple scattering theory, center by single scattering, right by modified single scattering theory with an additional phase factor and floated occupation number for the oxygen atoms.

metal–metal bonding, and it may serve as a possible fingerprint for polynuclear species.

The pre-edge feature varies markedly between the spectra in Figure 5. In the mononuclear anion **1** it is broader and weaker than in **2** and **3**. In $[Ru_3Co(CO)_{13}]^-$ it is particularly strong, as it is in other mixed metal clusters that we have recorded. It is virtually absent in the spectra of compounds with an oxygen donor set in an octahedral arrangement. This suggests that this feature is due to unoccupied 3d–4p hybrids, this mixing being forbidden in O_h symmetry. Changes in intensity may reflect the changes in the local site symmetry and possibly the number of metal–metal bonds to a cobalt center; this will increase the number of metal 4p containing states. In support of this, detailed molecular orbital

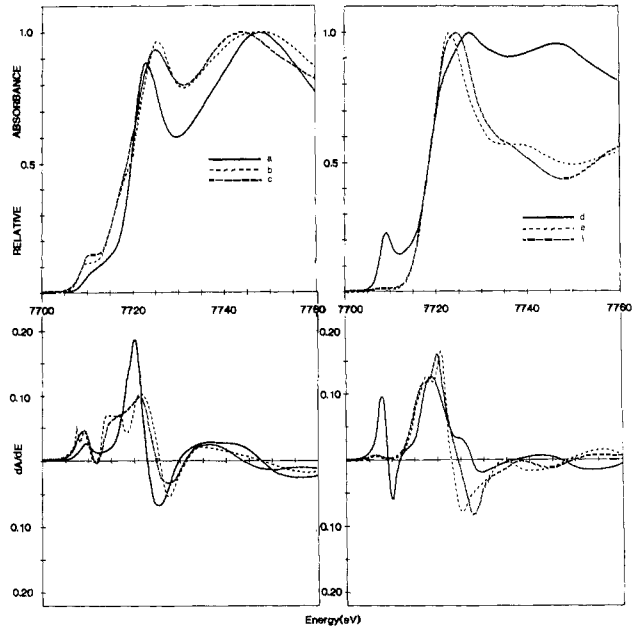

Figure 5. Near-edge structure (upper) and derivative (lower) for (a) $Co(CO)_4^-$, (b) $Co_3(CO)_9CH$, (c) $Co_4(CO)_{10}(PPh)_2$, (d) $Ru_3Co(CO)_{13}^-$, (e) an oxidized sample of $Co_3(CO)_9CSiCl_3$ on Al_2O_3, and (f) $Co(OH_2)_6^{2+}$.

calculations on molecular $CuCl_2$[41] and ME_4^{2-} ions (M = Cr, Mo; E = O, S)[40] indicate that the intensities of the alternative assignments of dipole-forbidden 1s–3d and 1s–4s transitions are negligible.

The pre-edge feature is ~9 eV to low energy of the edge position in $[Co(CO)_4]^-$ and 10–12 eV below the edge in the polynuclear complexes. These peaks are clearly composite, and higher resolution spectra of **2** show two distinct features. Pre-edge features in Cu^{2+} salts have been assigned to "shake-down" effects in which the 1s–4p transitions are accompanied by a ligand-to-metal charge transfer (LMCT) to form a $3d^{10}$ manifold in the excited state.[41] However, it was stated that, particularly in strongly covalent complexes (like carbonyls), it is more likely that satellites of this cause may appear to the high-energy side. Indeed Stern has reported such high-energy features in MCl_2 salts (M = Mn, Fe, and Ni).[42] This feature is absent in the Zn K-edge region of $KZnF_3$,[43] as anticipated if the LMCT process in the Cu^{II} complexes were to cause the completion of the 3d subshell. It is therefore extremely unlikely that this mechanism would give a low-energy satellite in complex **1**; a "frozen-orbital" description of the isoelectronic $Ni(CO)_4$ has shown that the $3d^{10}$ description is indeed a good starting point.[44]

Modelling the excited molecule using a $Z + 1$ atom or, better, a molecule containing the absorbing atom in this configuration is commonly adopted.[37] For example, the XANES features of manganese complexes have been treated in this way.[45] A prominent pre-edge absorption is apparent in $KMnO_4$ in particular, and this has been assigned as a transition to the t_2 orbitals consisting largely of manganese 3d character, but some 4p admixture; similar features have been explained in the chromate and the molybdate anions with the aid of SCF X_α calculations.[40] The first IP of $Ni(CO)_4$ is at ~9 eV,[46] and the UV-PES spectra of **2** and its derivatives have also been reported;[27,47] the first IP of $Co_3(C-$

(40) Kutzler, F. W.; Natoli, C. R.; Misemer, D. K.; Doniach, S.; Hodgson, K. O. *J. Chem. Phys.* **1980**, *73*, 3274.
(41) Bair, R. A.; Goddard, W. A., III *Phys. Rev. B* **1980**, *22*, 2767.
(42) Stern, E. A. *Phys. Rev. Lett.* **1982**, *49*, 1353.
(43) Schulman, R. G.; Yafet, Y.; Eisenberger, P.; Blumberg, W. E. *Proc. Natl. Acad. Sci.* **1976**, *73*, 1384.
(44) Bauschlicher, C. W., Jr.; Bagus, P. S. *J. Chem. Phys.* **1984**, *81*, 5889.
(45) Belli, M.; Scafati, A.; Bianconi, A.; Mobilo, S.; Palladino, L.; Reale, A.; Burattini, E. *Solid State Commun.* **1980**, *35*, 355.
(46) Eland, J. H. D. *Photoelectron Spectroscopy*; Butterworths: London, 1974.

Table IV. Correlations between Variables Associated with Major Shells Using Multiple Scattering Theory[a]

B. $Co_3(CO)_9CH$

	R_1	R_2	R_3	A_1	A_2	A_3	E_0
R_2	0.33						
R_3	0.36	0.42					
A_1	−0.05	−0.09	0.04				
A_2	0.20	0.08	0.27	0.07			
A_3	−0.01	−0.20	−0.06	0.03	−0.08		
E_0	−0.54	−0.58	−0.67	0.01	−0.18	0.02	
SB	0.05	0.01	0.07	−0.10	0.07	0.45	−0.06

C. $Co_4(CO)_{10}(PPh)_2$

	R_1	R_2	R_3	R_4	R_5	R_6	A_1	A_2	$A_{3/4}$	A_5	A_6	E_0
R_2	0.66											
R_3	0.69	0.52										
R_4	−0.19	0.17	−0.40									
R_5	0.69	0.57	0.86	−0.59								
R_6	0.32	0.25	0.41	−0.25	0.42							
A_1	0.19	0.41	0.08	0.15	0.16	0.05						
A_2	−0.61	−0.37	−0.88	0.49	−0.76	−0.35	−0.05					
$A_{3/4}$	−0.24	0.17	−0.58	0.93	−0.60	−0.29	0.21	0.64				
A_5	0.02	−0.31	0.14	−0.92	0.36	0.12	−0.15	−0.26	−0.79			
A_6	−0.00	0.01	0.03	0.10	−0.03	−0.04	−0.02	−0.01	0.06	−0.10		
E_0	−0.76	−0.66	−0.83	0.50	−0.94	−0.43	−0.20	0.74	0.52	−0.31	0.03	
SB	0.57	0.56	0.81	−0.15	0.70	0.36	0.07	−0.67	−0.33	−0.21	0.01	−0.64

[a] R_n and A_n refer to the distances and Debye–Waller factors for shell n. Shell sequence as for Table III. SB refers to the sine of the Co–C–O bond angles.

$O)_9CH$ is at 8.12 eV. So, on a one-electron model, the lowest energy vacant orbitals will be at substantially less negative energies. The energies of these orbitals in the excited state will be slightly lowered by the presence of the core hole; modelling by the $Z+1$ approximation indicates a lowering of the order of 1 eV,[48] while our Co atomic wave function calculations showed that the effect of the screened core hole was to reduce the orbital energy by less than this value. It therefore seems clear that the vacuum level in these complexes approximately corresponds to the onset of the rise of the absorption edge. Indeed calculations on MO_4^{2-} ions indicated that the onset of the continuum also occurred at the base of the K-absorption edge.[40]

Above the edge we see a marked contrast between the carbonyls which have a strong feature at around 7745 eV (which we have shown to have a strong oxygen multiple scattering contribution) and the other spectra. The other two are so similar as to suggest that the oxidized material is another hexaqua complex but with a slightly longer mean bond length and lower disorder than in the crystalline nitrate. Other spectra we have examined show all those with oxygen ligands to be broadly similar though not as close to the oxidized carbonyl as is the hexaqua compound.

Qualitative comparisions of edge spectra, which may be obtained very rapidly, may thus be of use in identifying species present in a sample even if the dilution or disorder in the material prevents data from being recorded in the EXAFS region. This technique would be of particular advantage in monitoring real-time studies of catalysts with energy dispersive measurements.

Conclusions

These analyses show that multiple scattering within carbonyl groups is the dominant contribution from the oxygen shell in linear carbonyl groups and also affects the backscattering within bridging carbonyls. By using a spherical wave formalism allowing for scattering of up to third order, then EXAFS data of carbonyl complexes can be fitted as close as 14 eV above the absorption edge and used to estimate the M–C–O bond angle. By taking due care of statistical criteria, valid multishell fits for metal cluster species can be obtained which provide considerable structural detail. For cobalt K-edges, the near-edge structure may be used as a fingerprint for particular cobalt environments.

Acknowledgment. We thak the SERC for support, S. L. Scruton for providing the sample of $PPN[Co(CO)_4]$, and Professor R. B. Bau for sending details of ref 13. We are grateful to Drs. S. J. Gurman and P. J. Durham for helpful discussions and Dr. I. Ross for the spectrum of $Co[OH_2]_6(NO_3)_2$.

Registry No. 1, 53433-12-8; **2**, 15664-75-2; **3**, 58092-22-1; **4**, 72152-11-5; **5**, 64115-57-7; **6**, 23730-86-1.

(47) Checky, P. T.; Hall, M. B. *Inorg. Chem.* **1981**, *20*, 4419. Desmukh, P.; Dutta, T. K.; Huang, J. L-S.; Housecroft, C. E.; Fehlner, T. P. *J. Am. Chem. Soc.* **1982**, *104*, 1740. DeKock, R. L.; Desmukh, P.; Dutta, T. K.; Fehlner, T. P.; Housecroft, C. E.; Huang, J. L.-S. *Organometallics* **1983**, *2*, 1108.

(48) Basch, H.; Viste, A.; Gray, H. B. *Theor. Chim. Acta* **1965**, *3*, 458.